Archival Report

Biological Psychiatry: GOS

Multidimensional Effects of Stress on Neuronal Exosome Levels and Simultaneous Transcriptomic Profiles

Hope Kronman, Amarjyot Singh, Shofiul Azam, Andrea S. Guzman, Danielle Zelli, Timothy Lau, Josh Dobbin, Benedetta Bigio, and Carla Nasca

ABSTRACT

BACKGROUND: An excess of exosomes, nanovesicles released from all cells and key regulators of brain plasticity, is an emerging therapeutic target for stress-related mental illnesses. The effects of chronic stress on exosome levels are unknown; even less is known about molecular drivers of exosome levels in the stress response.

METHODS: We used our state-of-the-art protocol with 2 complementary strategies to isolate neuronal exosomes from plasma, ventral dentate gyrus, basolateral amygdala, and olfactory bulbs of male mice to determine the effects of chronic restraint stress (CRS) on exosome levels. Next, we used RNA sequencing and bioinformatic analyses to identify molecular drivers of exosome levels.

RESULTS: We found that CRS leads to an increase in the levels of neuronal exosomes but not total (i.e., not neuronally enriched) exosome levels assayed in plasma and the ventral dentate gyrus, whereas CRS leads to a decrease in neuronal exosome levels but not total exosome levels in the basolateral amygdala. There was a further specificity of effects as shown by a lack of changes in the levels of neuronal exosomes assayed in the olfactory bulbs. In pursuit of advancing translational applications, we showed that acetyl-L-carnitine administration restores the CRS-induced increase in neuronal exosome levels assayed in plasma (the most accessible specimen). Furthermore, the CRS-induced changes in neuronal exosome levels in the ventral dentate gyrus and basolateral amygdala mirrored the opposite pattern of CRS-induced transcriptional changes in these key brain areas, with β-estradiol signaling as a potential upstream driver of neuronal exosome levels.

CONCLUSIONS: This study provides a foundation for future studies of new forms of local and distant communication in stress neurobiology by demonstrating specific relationships between neuronal exosome levels assayed in plasma and the brain and providing new candidate targets for the normalization of exosome levels.

https://doi.org/10.1016/j.bpsgos.2024.100401

A chronic excess of circulating exosomes, nanovesicles secreted from all cells including neurons, is among the neural mechanisms associated with stress-related disorders, including major depressive disorder (MDD) (1–4). Key features for understanding the role of exosomes in stress-related illnesses are that exosomes cross the blood-brain barrier, are released in the blood circulation, and express surface markers highly specific, although not exclusive, for the organ that released them, allowing the immunoprecipitation of subpopulations of exosomes from blood (5–8). Prior studies have shown that exosomes regulate synaptic pruning, neurogenesis, and circuit function (9–11)—all biological processes dependent on synaptic glutamate and regulated by chronic stress (12–14). Remarkably, the effects of chronic stress on exosome levels, particularly neuronal exosomes assayed in key brain areas, are unknown, and even less is known about the relationship between neuronal exosome levels assayed in brain areas and blood.

By employing an innovative technology to isolate total exosomes (i.e., not enriched for neurons) and neuronal exosomes from plasma, our group showed increased levels of neuronal but not total exosomes in patients with MDD (1). We also found in vivo molecular signatures of brain insulin resistance in clinical phenotypes of depression that were also characterized by decreased levels of acetyl-L-carnitine (LAC), a modulator of the $mGlu_2$ receptor (metabotropic glutamate receptor 2, an inhibitor of synaptic glutamate release) (1,15–18). Dysfunction of glutamatergic neurotransmission is a core feature of MDD (19). Prior studies have also shown that the release of exosomes is modulated by glutamatergic neurotransmission (20). Insights into brain-body interaction can be gained by understanding relationships between neuronal exosomes isolated from plasma and key brain areas in rodent models of chronic stress, a risk factor for major mental illnesses (19,21,22).

Here, we focused on 2 key brain areas, the ventral dentate gyrus (vDG) of the hippocampus and the basolateral amygdala (BLA), in response to 21 days of chronic restraint stress (CRS) because prior work showed that these brain areas are

ISSN: 2667-1743

regulated by CRS, which results in a chronic hyperactivity of glutamatergic transmission in the hippocampus along with dendritic shrinkage, while it leads to dendritic elongation of BLA neurons (12,13,23). Opposite patterns of stress-induced changes in specific genes, such as BDNF (brain-derived neurotrophic factor), were also reported in these brain areas (24). Furthermore, while a vast literature has described the effects of several types of chronic stress paradigms on gene expression of a single brain area, less is known about simultaneous transcriptomic changes in these 2 stress-sensitive brain areas. Greater understanding of molecular pathways can provide new target candidates to regulate exosome levels that are altered in a variety of diseases (1–4).

In the current work, we used 2 complementary strategies for exosome isolation to determine 1) CRS effects on total (not neuronally enriched) and neuronal exosome levels assayed in key brain areas (i.e., vDG and BLA; olfactory bulbs [Obs] were used as a control area) and in plasma, 2) whether neuronal exosome levels assayed in plasma map onto neuronal exosome levels assayed in brain tissue, and 3) whether administration of LAC, an epigenetic modulator of glutamatergic function (15,16,25), ameliorates CRS effects on exosome levels assayed in plasma (the most accessible specimen). We also used RNA sequencing (RNA-seq) and bioinformatic analyses to identify simultaneous transcriptomic profiles within the vDG and BLA in stress responses and to begin mapping those pathways that may be upstream drivers of exosome levels.

METHODS AND MATERIALS

All procedures were carried out in accordance with the guidelines for animal care of the National Institutes of Health, the Institutional Animal Care and Use Committee of Rockefeller University, and Nathan Kline Institute for Psychiatric Research. See Supplemental Methods for details of the stress paradigm, pharmacological approach, exosome isolation, validation and quantification, RNA-seq assays and bioinformatic analyses, and statistical analysis.

RESULTS

Site-Specific Regulation of Neuronal, but Not Total, Exosome Levels by Chronic Stress in Plasma, vDG, BLA, and Obs

Driven by prior findings showing that the release of exosomes is modulated by synaptic glutamatergic activity (20), we began by screening total (not enriched for neurons) and neuronal exosome levels in plasma and 2 key brain areas, the vDG and BLA, in response to chronic stress. We used a stress paradigm of 21 days of CRS, a duration that has been demonstrated to lead to differential patterns of changes in dendritic plasticity in the ventral hippocampus and the connected BLA (12,13,23). We used an established approach to isolate exosomes followed by immunoprecipitation of neuronal exosomes from plasma and brain tissue of CRS mice and age-matched not-stressed male mice. This protocol allowed us to achieve high-throughput, quantitative isolation of exosomes from plasma and small brain areas (Figure 1A).

Three independent big datasets—the HPA (Human Protein Atlas), GTEx (Genotype-Tissue Expression) Project, and FANTOM5 (Functional Annotation of the Mammalian Genome 5) Consortium (26–28)—corroborate the use of L1CAM as a marker to enrich for the brain by showing that this protein is predominantly, although not exclusively, expressed in the brain, including the hippocampus, amygdala, and Obs (Figure S1), with negligible expression in peripheral organs (Figure 1B). Within the brain, L1CAM expression is high in neurons versus other cell types as shown by publicly available bulk RNA-seq (Figure 1C) and single-cell RNA seq from mouse brain areas (Figure 1D) (29,30). Expression array experiments confirmed the accuracy of the exosome purification and excluded potential contamination from cellular vesicles by showing: 1) robust staining of several known exosomal markers, such as TGS101, ANXA5, EPCAM, CD63, CD81, ALIX, ICAM, and FLOT; and 2) negligible staining for GM130, a marker of *cis*-Golgi vesicles (Figure 2A and Figure S2).

After CRS, no differences were observed in total exosome levels in plasma between the CRS group and the not-stressed control (Ctrl) group ($p = .6$, Ctrl [$n = 8$]: 19.4×10^9 ng/mL $\pm$ 1.2; CRS [$n = 10$]: 18.4×10^9 ng/mL $\pm$ 1.1) (Figure 2B). Using the same assay, we found a robust CRS-induced increase in L1CAM$^+$ exosome levels assayed in plasma ($p = .01$, Ctrl [$n = 8$]: 6.9×10^9 ng/mL $\pm$ 0.3; CRS [$n = 10$]: 7.7×10^9 ng/mL $\pm$ 0.1) (Figure 2C). To address direct regulation of exosome levels in the vDG, we isolated L1CAM$^+$ and total exosomes using vDG tissue. We found that vDG L1CAM$^+$ exosome levels differed significantly between CRS mice and not-stressed control mice, with mean counts being higher in the CRS group ($p = .02$, Ctrl [$n = 7$]: 8.4×10^9 ng/mL $\pm$ 0.2; CRS [$n = 9$]: 9.6×10^9 ng/mL $\pm$ 0.3) (Figure 2E); no change was found in vDG total exosomes ($p = .5$, Ctrl [$n = 7$]: 11.7×10^9 ng/mL $\pm$ 0.7; CRS [$n = 6$]: 11×10^9 ng/mL $\pm$ 0.6) (Figure 2D). No differences were observed in either L1CAM$^+$ or total exosome levels isolated from the Obs (total: $p = .9$, Ctrl [$n = 7$]: 11.6×10^9 ng/mL $\pm$ 0.9; CRS [$n = 6$]: 11.4×10^9 ng/mL $\pm$ 0.3; L1CAM$^+$: $p = .8$, Ctrl [$n = 7$]: 9.8×10^9 ng/mL $\pm$ 0.5; CRS [$n = 8$]: 9.6×10^9 ng/mL $\pm$ 0.4) (Figure 2F, G).

Given prior findings of opposite plasticity of the hippocampus and BLA after stress (23,31), we extended our exosome analyses to the BLA. We found a decrease in L1CAM$^+$ exosome levels but not total exosome levels in the BLA of CRS mice versus not-stressed control mice (L1CAM$^+$: $p < .0001$, Ctrl [$n = 7$]: 9.6×10^9 ng/mL $\pm$ 0.2; CRS [$n = 8$]: 8.3×10^9 ng/mL $\pm$ 0.2; total: $p = .2$, Ctrl [$n = 7$]: 10.4×10^9 ng/mL $\pm$ 0.3; CRS [$n = 6$]: 9.8×10^9 ng/mL $\pm$ 0.4) (Figure 2I, H). The violin plots depicted in Figure S3 summarizes the specificity of CRS effects on neuronal exosome levels in plasma and across these brain areas. The opposite pattern of changes in exosome levels in the vDG versus the BLA after CRS is consistent with prior findings of divergent structural remodeling in stress responses in these brain areas (12,13,23,31).

A Second Strategy for Neuronal Exosome Isolation Corroborates the Relationship Between Neuronal Exosome Levels in Plasma and the vDG

To corroborate the findings described above of a relationship between the increased levels of neuronal (L1CAM$^+$) exosomes assayed in plasma and the vDG, we extended our analysis using an additional exosome surface marker, NrCAM, to

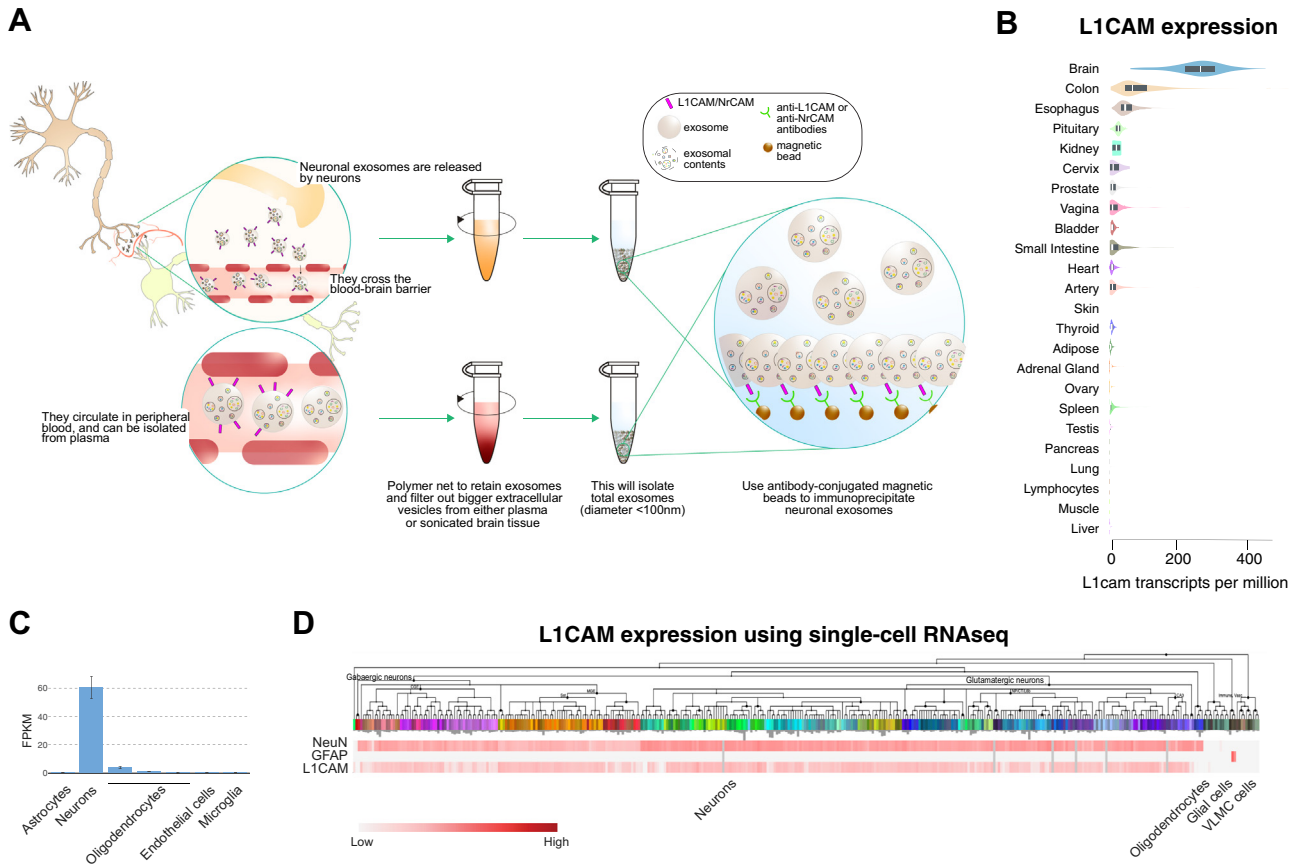

Figure 1. Neuronal exosome immunoprecipitation from plasma or brain tissue. **(A)** Model featuring exosome biology and polymer net followed by antibody-based technology for the isolation of total (i.e., not enriched for neurons) and neuronal exosomes from plasma or brain tissue. Exosomes are nanovesicles of endosomal origin that are secreted from all cells including neurons; they cross the blood-brain barrier and are released in the circulation. Exosomes express surface markers, including L1CAM or NrCAM (also see Figure 3), that are highly specific, although not exclusively, to the organ that releases them. Total exosomes can be purified from plasma or brain tissue, and exosome subpopulations can be isolated from these total exosomes by immunoprecipitation with magnetic beads conjugated to antibodies for proteins that are expressed in the organ of interest (i.e., the brain). **(B)** Publicly available databases (e.g., The Human Protein Atlas, https://www.proteinatlas.org/) show that L1CAM is a protein highly expressed in the brain, with minimal expression in peripheral organs. **(C)** L1CAM is highly expressed in neurons compared with other cell types of the brain as shown by FPKM using an independent bulk RNA-seq database of glia, neurons, and other cells. Also see Figure S1, which shows robust and high expression of L1CAM in the hippocampus, amygdala, and olfactory bulbs. **(D)** Single-cell RNA-seq data from the Allen Brain Atlas further corroborate high and robust expression of L1CAM in neurons compared with other cells of the brain (e.g., astrocytes). GFAP (a marker that is highly expressed in astrocytes) and NeuN (a marker that is highly expressed in neurons) expression levels are also reported as a comparison. FPKM, fragments per kilobase of transcript per million mapped reads; RNAseq, RNA sequencing.

isolate neuronal exosomes and test our prediction that CRS would lead to an increase in NrCAM$^+$ exosome levels assayed in plasma and the vDG. Three large, independent datasets (HPA, GTEx, and FANTOM5) (26–28) and single-cell RNA-seq data from mouse hippocampus and cortex (Allen Brain Atlas) (30) showed high and robust expression of NrCAM in the brain (Figure 3A), particularly in glutamatergic neurons (Figure 3B). The expression of NrCAM is also mutually exclusive with L1CAM expression: L1CAM showed some although negligible expression in the colon and esophagus, while NrCAM expression was absent. Furthermore, NrCAM showed some although negligible expression in adrenal glands, while L1CAM expression was absent; both markers showed negligible expression in other peripheral organs (e.g., pituitary or kidney) compared with the brain. Consistent with our prediction of a CRS-induced increase in neuronal exosome levels as also shown by the L1CAM findings above, we found an increase in neuronal (NrCAM$^+$) exosome levels isolated from both plasma and the vDG of CRS mice versus not-stressed control mice (plasma: $p = .04$, Ctrl [$n = 6$]: 8.8×10^9 ng/mL $\pm$ 0.1; CRS [$n = 8$]: 9.5×10^9 ng/mL $\pm$ 0.3; vDG: $p = .0001$, Ctrl [$n = 7$]: 8.6×10^9 ng/mL $\pm$ 0.1; CRS [$n = 9$]: 9.7×10^9 ng/mL $\pm$ 0.2) (Figure 3C, D). Collectively, these results using 2 complementary markers corroborate the finding of a relationship between plasma and vDG neuronal exosome levels and provide greater cellular and topographical specificity for future translational research.

Administration of LAC Restores CRS-Induced Increase in Plasma Neuronal Exosome Levels: Translational Implications

Driven by the prior discovery of increased neuronal exosome levels in plasma of patients with MDD characterized by a

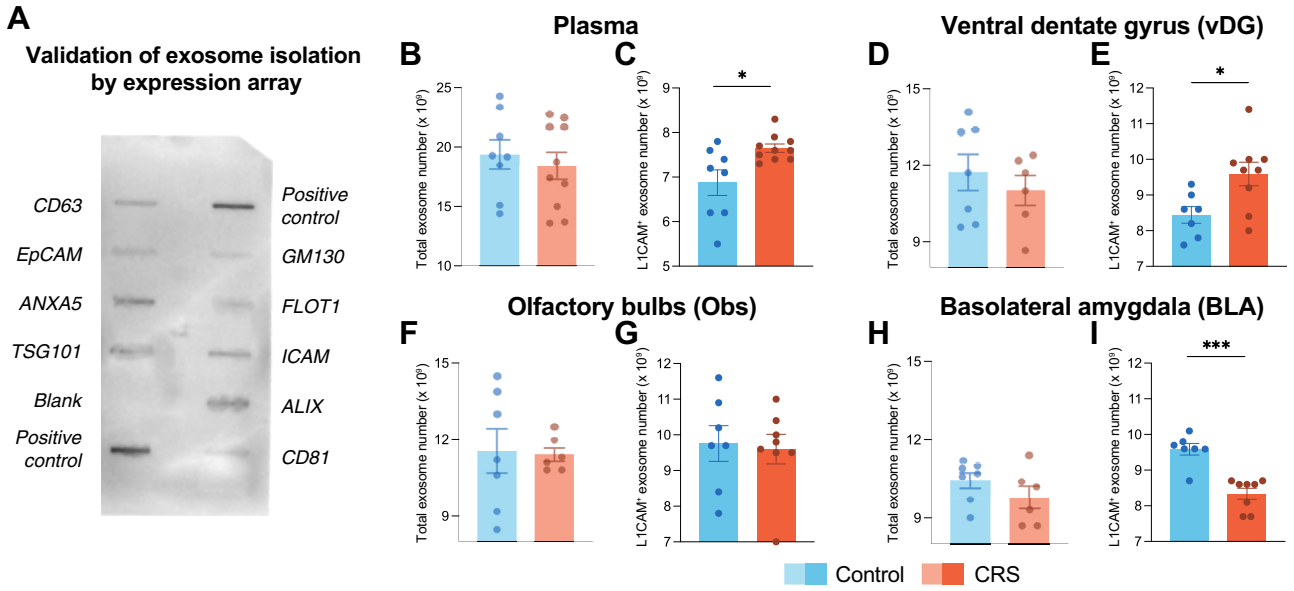

Figure 2. Site-specific regulation of neuronal exosome levels, but not total exosome levels, by chronic stress in plasma, the vDG of the hippocampus, olfactory bulbs, and basolateral nucleus of the amygdala. **(A)** Validation and accuracy of exosome isolation: expression array validated the accuracy of the exosome isolation as shown by strong staining of positive controls and a combination of multiple known exosomal markers (CD63, EPCAM, ANXA5, TSG101, FLOT, ICAM, ALIX, CD81), while also confirming the exclusion of cellular contamination from cellular vesicles as shown by negligible staining for GM130, a marker for *cis*-Golgi vesicles. Also see Figure S2. **(B, C)** CRS-induced increase in the levels of neuronal ($L1CAM^+$) but not total exosomes assayed in plasma: no differences were observed in the levels of total exosomes assayed in plasma between CRS mice and not-stressed control mice [**(B)** $p = .6$, Ctrl ($n = 8$): 19.4×10^9 ng/mL ±1.2; CRS ($n = 10$): 18.4×10^9 ng/mL ± 1.1]. CRS resulted in an increase in the levels of neuronal ($L1CAM^+$) exosomes isolated from plasma compared with age-matched not-stressed control mice [**(C)** $p = .01$, Ctrl ($n = 8$): 6.9×10^9 ng/mL ± 0.3; CRS ($n = 10$): 7.7×10^9 ng/mL ± 0.1]. Using this same technology for exosome isolation and count, our previous studies showed increased levels of neuronal ($L1CAM^+$) exosomes, but not total exosomes, assayed in plasma of patients with MDD compared with age- and sex-matched control subjects. **(D, E)** CRS-induced increase in the levels of neuronal ($L1CAM^+$) but not total exosomes isolated from vDG tissue: no differences were observed in the levels of total exosomes in vDG tissue between the CRS and control groups [**(D)** $p = .5$, Ctrl ($n = 7$): 11.7×10^9 ng/mL ± 0.7; CRS ($n = 6$): 11×10^9 ng/mL ± 0.6]. Similar to the increase in neuronal exosome levels assayed in plasma, CRS resulted in an increase in the levels of neuronal ($L1CAM^+$) exosomes isolated from vDG compared with age-matched not-stressed control mice [**(E)** $p = .02$, Ctrl ($n = 7$): 8.4×10^9 ng/mL ± 0.2; CRS ($n = 9$): 9.6×10^9 ng/mL ± 0.3]. **(F, G)** Levels of total and neuronal ($L1CAM^+$) exosomes isolated from the control brain area, the Ob: no differences were observed in the levels of either total or neuronal ($L1CAM^+$) exosomes isolated from the Ob between the CRS and control groups [**(F)** $p = .9$, Ctrl ($n = 7$): 11.6×10^9 ng/mL ± 0.9; CRS ($n = 6$): 11.4×10^9 ng/mL ± 0.3; **(G)** $p = 0.8$, Ctrl ($n = 7$): 9.8×10^9 ng/mL ± 0.5; CRS ($n = 8$): 9.6×10^9 ng/mL ± 0.4]. **(H, I)** Levels of total and neuronal ($L1CAM^+$) exosomes isolated from BLA tissue: no differences were observed in the levels of total exosomes in BLA tissue between the CRS and control groups [**(H)** $p = 0.2$, Ctrl ($n = 7$): 10.4×10^9 ng/mL ± 0.3; CRS (n = 6): 9.8×10^9 ng/mL ± 0.4]. CRS resulted in a decrease in the levels of neuronal ($L1CAM^+$) exosomes isolated from the BLA compared with age-matched not-stressed control mice [**(I)** $p < .0001$, Ctrl ($n = 7$): 9.6×10^9 ng/mL ± 0.2; CRS ($n = 8$): 8.3×10^9 ng/mL ± 0.2]. Bars represent mean ± SEM. Asterisks indicates significant comparisons with not-stressed control group. $^*p < .05$, $^{***}p < .001$ at 2-tailed Student's *t* tests as appropriate. CRS, chronic restraint stress.

deficiency of LAC, and because plasma is the most accessible specimen particularly in clinical settings, we tested the hypothesis that administration of LAC would restore both $NrCAM^+$ and $L1CAM^+$ exosome levels in plasma of CRS mice to the levels of not-stressed control mice. After 3 days of administration of LAC, a dose that leads to a rapid antidepressant-like response in multiple chronic stress paradigms, including CRS (15,16,25,32), we found no difference in plasma $NrCAM^+$ and $L1CAM^+$exosome levels between the CRS group that received LAC and the not-stressed control group ($NrCAM^+$: $F_{1,20} = 20.2$, $p < .001$ [stress]; $F_{1,20} = 24.3$, $p < .001$ [treatment]; $F_{1,20} = 0.9$, $p = .4$ [interaction]; $L1CAM^+$: $F_{1,18} = 9.3$, $p < .01$ [stress]; $F_{1,18} = 2$, $p = .2$ [treatment]; $F_{1,18} = 1.3$, $p = .3$ [interaction]) (Figure 4A, B). We also found a decrease in $NrCAM^+$ exosome levels in not-stressed control mice that received LAC. These findings are consistent with previous studies reporting a link between increased synaptic glutamatergic activity and increased exosome levels, an effect that we show is blocked by administration of the epigenetic modulator of glutamatergic function LAC after chronic stress.

Stress-Induced Transcriptional Changes in the vDG and BLA Mirror the Directionality of Changes in the Levels of Neuronal Exosomes: β-Estradiol Signaling as a Potential Upstream Driver of Exosome Levels

Next, we hypothesized that the CRS-induced opposite pattern of changes in neuronal exosome levels in the vDG and BLA is suggestive of differential regulation of gene expression in these mood-regulatory brain areas. We used RNA-seq and bioinformatic analyses to capture simultaneous transcriptome-wide alterations in the vDG and BLA tissue after CRS versus age-matched not-stressed control mice (Figure 5) to begin to identify the genes and molecular pathways that contribute to exosome levels in stress responses. We used a total of 9 mice for each group, and 3 mice with the same vulnerability and

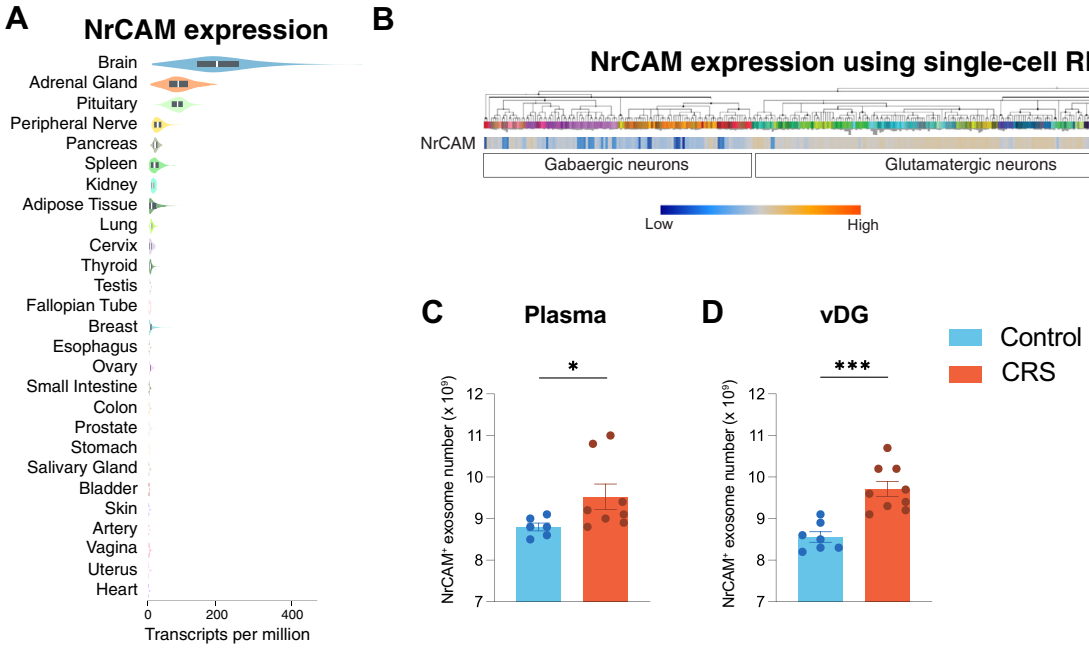

Figure 3. A second approach for exosome isolation corroborates the relationship between neuronal exosome levels in plasma and the vDG of the hippocampus. **(A)** Publicly available databases (e.g., The Human Protein Atlas, https://www.proteinatlas.org/) show that NrCAM is a protein with high and robust expression in the brain and negligible expression in peripheral organs. The expression of NrCAM is also mutually exclusive with the expression of L1CAM in the top 2 peripheral organs: L1CAM shows negligible expression in the colon and esophagus, while NrCAM expression is absent. Conversely, NrCAM shows negligible expression in the adrenal glands, while L1CAM expression is absent; both markers show negligible expression in other peripheral organs (e.g., pituitary or kidney) compared with the brain. **(B)** Single-cell RNA-seq data from the Allen Brain Atlas show high and robust expression of NrCAM in glutamatergic neurons. **(C, D)** Levels of neuronal ($NrCAM^+$) exosomes assayed in plasma and vDG tissue after CRS: as we hypothesized, CRS resulted in an increase in the levels of neuronal exosomes assayed in both plasma and vDG tissue compared with age-matched not-stressed control mice [**(C)** $p = .04$, Ctrl ($n = 6$): 8.8×10^9 ng/mL ± 0.1; CRS ($n = 8$): 9.5×10^9 ng/mL ± 0.3; **(D)** $p = .0001$, Ctrl ($n = 7$): 8.6×10^9 ng/mL ± 0.1; CRS ($n = 9$): 9.7×10^9 ng/mL ± 0.2]. In addition to corroborate the relationship between neuronal exosomes assayed in plasma and vDG tissue with the use of L1CAM, these findings provide a tool with greater cellular and topographical specificity that can be used in future translational research. Bars represent mean ± SEM. Asterisks indicates significant comparisons with the not-stressed control group. $^*p < .05$, $^{***}p < .001$ at 1-tailed Student's *t* tests as appropriate. CRS, chronic restraint stress; RNAseq, RNA sequencing; vDG, ventral dentate gyrus.

phenotype were pooled together to yield the proper amount of RNA per sample in each of the 3 biological replicates of each group, as we and others described in prior papers (15,33). First, we assessed the quality of the transcriptomic data after the initial filtering and normalization steps of the differential expression analysis. Volcano plot analyses showed a robust number of genes that reached the designated fold change (FC) and significance cutoffs (false discovery rate [FDR] ≤ 0.15, FC > 1.3, $\log_2$FC > 0.4) (Figure 5A, B). We also used unsupervised principal component analysis to cluster individual samples for the vDG and BLA RNA-seq data. This analysis reduces variables within high-dimensional transcriptional data by transforming a large number of transcript changes into single variables or principal components (PCs) and depicting samples on a coordinate system based on these specific PCs (Figure 5C, D). Principal component analysis of the vDG RNA-seq data showed a clear separation between the CRS and control groups based on a map from the top 3 PCs, i.e., PC1, PC2, and PC3 (Figure 5C); a similar separation of the CRS and control groups was obtained using BLA-specific PC1, PC2, and PC3 (Figure 5D). CRS mice were characterized by depressive-like behaviors as shown by a decrease in social interactions, abnormal coping style test, and anhedonia-like behavior as previously shown by our and other groups (15,23,34,35). Taken together, these data indicate that the RNA-seq data for these 2 stress-sensitive brain areas captured meaningful transcriptomic changes in phenotypes of chronic stress.

We found that CRS results in a differential regulation of gene expression in the vDG and BLA, with a pattern of more pronounced transcriptomic changes and >3 times as many differentially expressed genes in the vDG versus the BLA (Figure 5A, B, circles). We found altered expression of 395 genes with 236 upregulated and 159 downregulated genes in the vDG of CRS versus not-stressed control group and a different pattern of changes with the differentially expressed genes preferentially downregulated (90 downregulated, 25 upregulated) and a smaller number of transcriptomic changes in the BLA than the vDG using the same cutoffs. These data showed a remarkable directionality of transcriptomic changes that parallel the changes observed in neuronal exosome levels after CRS in these 2 brain areas.

Using enrichment and Gene Ontology (GO) analyses on the differentially expressed transcripts, we showed that CRS altered multiple relevant signaling pathways in the vDG and BLA (Figure 6 and Table S1). In both brain areas, bioinformatic analyses showed meaningful gene categories related to

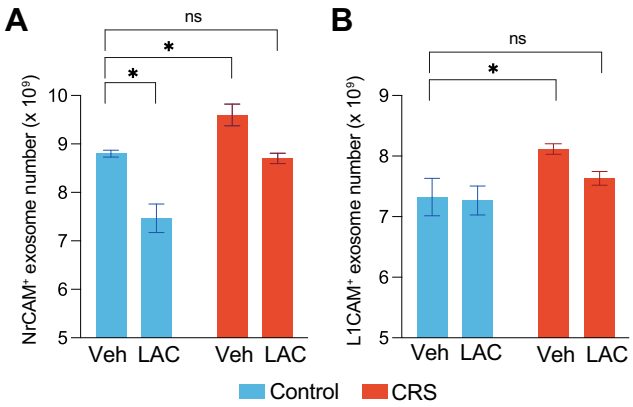

Figure 4. Administration of LAC restores CRS-induced increase in plasma neuronal exosome levels: translational implications. Administration of LAC restores the CRS-induced increase in both **(A)** NrCAM+ and **(B)** L1CAM+ exosome levels in plasma to the levels of not-stressed control mice: no difference in the levels of plasma neuronal exosomes between the CRS group that received LAC and the not-stressed control group [**(A)** $F_{1,20}$ = 20.2, $p < .001$ (stress); $F_{1,20}$ = 24.3, $p < .001$ (treatment); $F_{1,20}$ = 0.9, $p = .4$ (interaction); **(B)** $F_{1,18}$ = 9.3, $p < .01$ (stress); $F_{1,18}$ = 2, $p = .2$ (treatment); $F_{1,18}$ = 1.3, $p = .3$ (interaction)]. Our previous work showed increased neuronal exosomes assayed in plasma—the most accessible biospecimen in the clinical setting—of patients with major depressive disorder characterized by a deficiency of LAC, an epigenetic modulator of glutamatergic function. These findings are also akin to previous studies that reported a link between higher release of exosomes and increased synaptic glutamatergic activity. Asterisk indicates significant comparisons with the not-stressed control group, *$p < .05$ at Holm-Sídák's post hoc test to control for multiple comparisons. Bars represent mean ± SEM. CRS, chronic restraint stress; LAC, acetyl-L-carnitine; ns, not significant.

dendritic remodeling, neuron projection, and extracellular matrix compartments consistent with prior research showing extensive structural changes in the ventral hippocampus and BLA after prolonged chronic stress (13,23,31,36). In the vDG, a particularly meaningful gene category was related to insulin signaling pathways (Figure 6A), with upregulation of *Igf2* (FC = 1.74, FDR = 2.2×10^{-4}) and *Lrp2* (FC = 2.40, FDR = 2.0×10^{-3}), as well as insulin-like growth factor proteins *Igfbp2* (FC = 2.20, FDR = 3.13×10^{-8}) and *Igfbp3* (FC = 1.61, FDR = .02). There was a downregulation of *Igfbp6* (FC = 0.42, FDR = 4.28×10^{-7}), *Rxfp1* (FC = 0.59, FDR = 4.5×10^{-4}), and *Glp2r* (FC = 0.58, FDR = 7.8×10^{-3}). The current findings are also akin to prior studies that showed robust changes in key markers of the insulin signaling cascade in the vDG of rodent models with depressive-like behavior as well as in the molecular cargo of L1CAM$^+$ exosomes isolated from plasma of patients with MDD (1,37). Our bioinformatic analyses and RNA-seq road maps of these 2 brain areas expand current literature on the effects of CRS on suppressing expression of key glutamate genes in the vDG, the $mGlu_2$ receptor and the glial glutamate exchanger xCT (15), and provide a simultaneous transcriptomic characterization of the vDG and BLA in the aftermath of chronic stress that will be an important reservoir for future studies aimed at understanding the role of exosomes in stress neurobiology.

Lastly, to address potential regulation of neuronal exosome levels through molecular targets and mechanisms, we used a complementary bioinformatic approach to disentangle those specific overlapping molecular pathways between the vDG and BLA and the upstream regulators that may account for common mechanisms across the 2 brain areas. We found 43

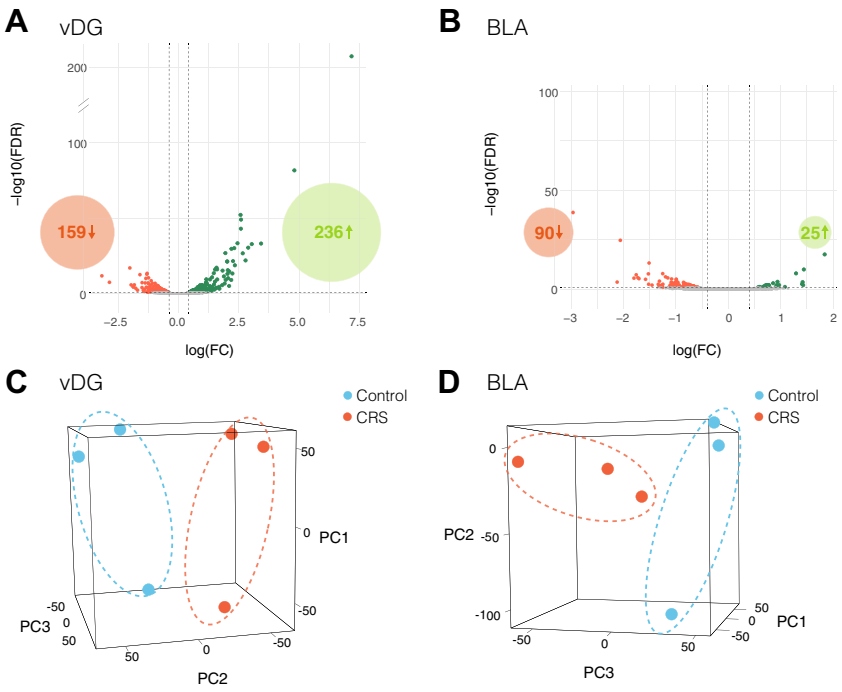

Figure 5. High quality RNA sequencing data carries a signal that separates the CRS group from the not-stressed control group. **(A)** Volcano plot of transcripts in the vDG with cutoffs of FDR ≤ 0.15 ($-\log_{10}$(FDR) ≥ 0.83) and FC > 1.3 ($\log_2$FC < 0.4). Insets show the total number of up- and downregulated genes that meet these cutoffs (236 upregulated, 159 downregulated). **(B)** Volcano plot of transcripts in the BLA with cutoffs of FDR ≤ 0.15 ($-\log_{10}$(FDR) ≥ 0.83) and FC > 1.3 ($\log_2$FC < 0.4). Insets show the total number of up- and downregulated genes that meet these cutoffs (25 upregulated, 90 downregulated). **(C)** PCA of vDG samples based on read counts showing separation of control and CRS samples by the top 3 principal components (PC1, PC2, and PC3). **(D)** PCA of BLA samples based on read counts showing separation of control and CRS samples by the top 3 principal components (PC1, PC2, PC3). BLA, basolateral amygdala; CRS, chronic restraint stress; FC, fold change; FDR, false discovery rate; PCA, principal component analysis; vDG, ventral dentate gyrus.

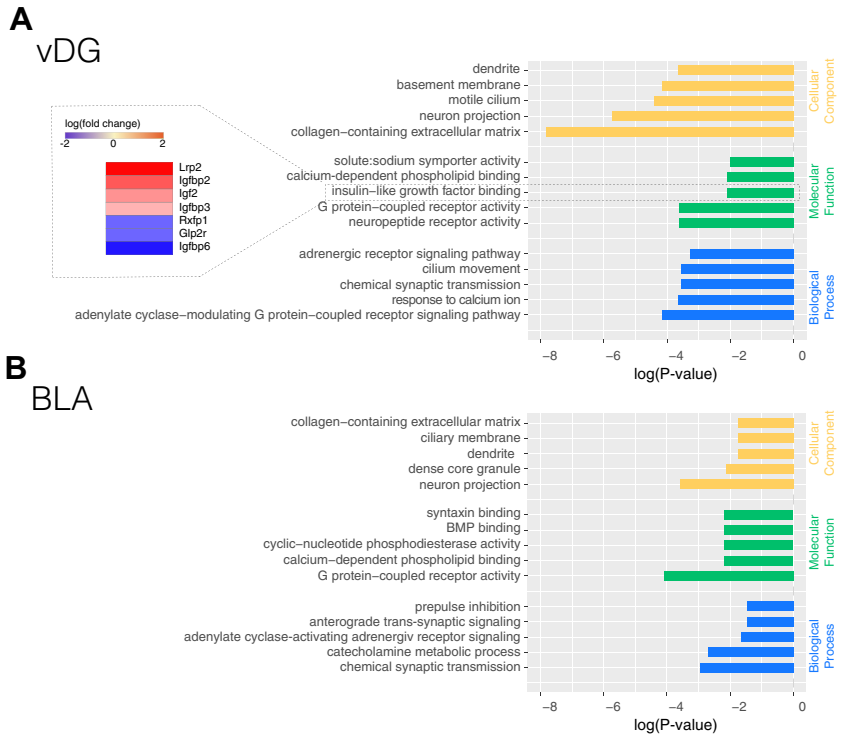

Figure 6. GO analysis of differentially expressed genes from the vDG and BLA. **(A)** Log(adjusted *p* value) of enriched GO terms in the vDG showing top 5 not-redundant terms per category (cellular component, molecular function, biological process) with not-redundant transcripts. Inset is heatmap of genes involved in "insulin-like growth factor binding" (GO:0031994). **(B)** Log(adjusted *p* value) of enriched GO terms in the BLA, showing the top 5 terms per category (cellular component, molecular function, biological process) with not-redundant transcripts. BLA, basolateral amygdala; BMP, bone morphogenetic protein; GO, Gene Ontology; vDG, ventral dentate gyrus.

overlapping differentially expressed genes between the 2 brain areas, with largely opposite patterns of regulation (Figure 7A and Table S2). In fact, when these genes were clustered, 33 of them fell into a cluster showing predominantly opposite directionality, with most genes upregulated in the vDG and all of them downregulated in the BLA. This pattern mirrored changes in neuronal exosome levels in these same brain areas. Notably, the most relevant term generated by cellular component GO analysis was secretory/exocytic vesicles (Figure 7B).

Next, we performed upstream regulator analysis to predict those signaling pathways that may be upstream of the changes to the overlapping 43 transcripts between the vDG and BLA. As shown by the heatmap of upstream regulators depicting *z* score of prediction (Figure 7C), we found that the predictions were largely in opposite directions in the vDG and BLA, consistent with the inverse directionality of differentially expressed genes loaded into the upstream analysis. Notably, the upstream regulator pathway with the largest *z* score across the 2 areas was β-estradiol signaling (Figure 7D), which is consistent with prior findings of a link between β-estradiol signaling and stress-dependent structural changes (38–42) and other findings suggesting that the secretion of exosomes is modulated by estradiol (43,44). Interestingly, β-estradiol signaling was also the only upstream regulator predicted to regulate synaptotagmins *Syt2* and *Syt6*, the 2 transcripts responsible for the GO enrichment for secretory/exocytic vesicles. This study provides a conceptual template for future studies aimed at characterizing the connection between estradiol-related transcriptional networks and exosome biology in the response to stress.

DISCUSSION

In this study, we reported increased levels of neuronal exosomes assayed in plasma of mice after chronic stress, an effect that we have previously shown in patients with MDD (1). We also reported a specificity of changes in the levels of neuronal exosomes in that we found no changes in the levels of total exosomes (i.e., exosomes not enriched for neurons) and that the changes in neuronal exosomes assayed in plasma reflect the levels of neuronal exosomes directly assayed in the vDG of the hippocampus but not in the brain area Obs. To advance translational applications of neuronal exosome analysis using plasma (the most accessible specimen for translational research), our data also showed an amelioration of CRS-induced increase in neuronal exosome levels assayed in plasma after administration of LAC. Furthermore, our data showed an opposite pattern of CRS-induced changes in neuronal exosome levels between the vDG and BLA that mirrored transcriptional changes in these 2 brain areas and pointed to β-estradiol signaling as an upstream driver of the effects of chronic stress on neuronal exosome levels.

The stress-induced increase in neuronal ($L1CAM^+$ and $NrCAM^+$) exosome levels assayed in both plasma and vDG tissue is important because exosome levels are altered in a variety of diseases, and exosomes are regulatory mechanisms of brain plasticity (1–4,10,11). Furthermore, no significant effect

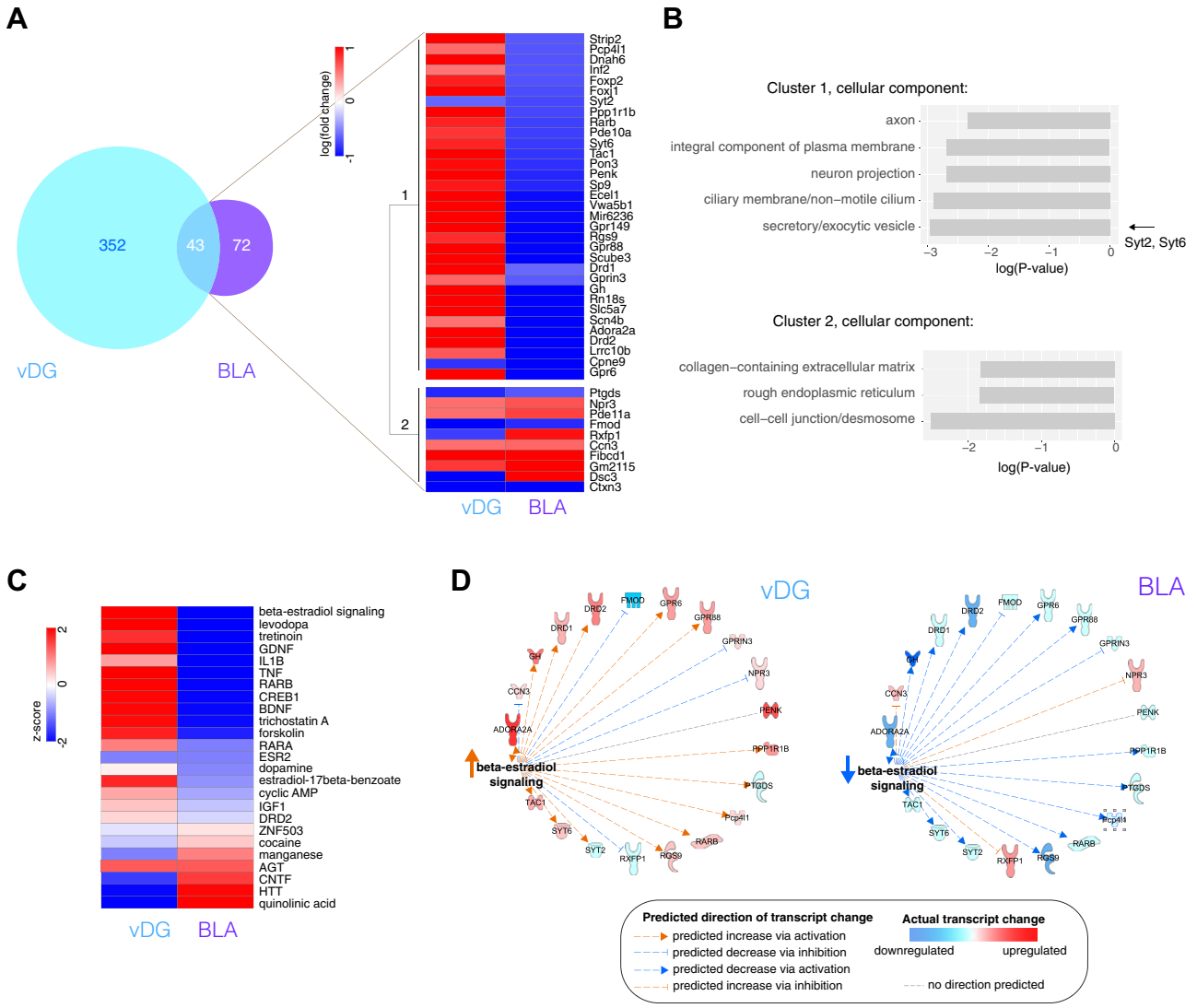

Figure 7. Potential neuronal exosome regulation through estradiol signaling in male mice. **(A)** Venn diagram of the 43 overlapping differentially expressed genes between the vDG and BLA after chronic restraint stress and heatmap of their expression showing 2 clusters of transcripts generated by hierarchical clustering (cluster 1 and cluster 2). **(B)** Gene Ontology cellular component enrichment of the 2 clusters of transcripts. Cluster 1 enriches for secretory/exocytic vesicles based on the inclusion of synaptotagmins *Syt2* and *Syt6*. **(C)** Heatmap of upstream regulators predicted to regulate the 43 overlapping transcripts in each area (*z* score is shown). **(D)** β-estradiol signaling networks generated by Ingenuity Pathway Analysis from the 43 overlapping genes. In the vDG network (left), β-estradiol signaling is predicted to increase upstream of the transcripts in the network; the orange arrows indicate a predicted increase of the target transcript, while the blue inhibiting lines indicate a predicted decrease. In the BLA network (right), β-estradiol signaling is predicted to decrease upstream; the blue arrows indicate a predicted decrease of the target transcript (β-estradiol signaling normally increases the target, but with β-estradiol signaling down-regulated, the target molecule decreases), while the orange inhibiting lines indicate a predicted increase (β-estradiol signaling normally inhibits the target, but with β-estradiol signaling downregulated, the target molecule increases). Targets are colored according to their actual change in the RNAseq, with blue indicating downregulation and orange indicating upregulation. Fifteen of 20 transcripts in the vDG network and 19 of 20 in the BLA network show actual RNAseq changes in the same direction of prediction. BLA, basolateral amygdala; RNAseq, RNA sequencing; vDG, ventral dentate gyrus.

of CRS was found in total exosomes (i.e., not enriched for neurons) or in the levels of neuronal exosomes in the Obs brain area. Using this same technology, we previously showed an increase in the levels of neuronal exosomes in patients with MDD compared with age- and sex-matched control subjects (1). We also reported a brain metabolic dysfunction known as insulin resistance as shown by an increased expression of the insulin-docking protein IRS1, a molecular hub that propagates the insulin signaling cascade, in depression (1). Prior work has shown a widespread localization of molecular markers of the insulin signaling pathway in brain areas key for mood and cognition, including the hippocampal subregions (45,46). The insulin signaling pathway was consistently among the top 5 gene categories in the GO analysis, with meaningful changes in molecular markers such as *Igf2* and *Lpr2* in the vDG of the hippocampus of CRS mice compared with not-stressed

control mice. Therefore, the animal models provide a conceptual platform that is consistent with the role of brain insulin resistance among other mediators of allostatic load (glutamatergic dysfunction, altered trophic environment, and inflammatory states) in humans with depression (12,47–51). Collectively, these 2 complementary strategies strongly support a relationship between central (vDG) and peripheral (plasma) neuronal exosome levels, and the use of NrCAM provides greater cellular specificity to the utility of plasma neuronal exosome analysis.

A potential biological underpinning of the observed stress-induced increase in neuronal exosomes in the vDG may be that the overflow of synaptic glutamate in the hippocampus after CRS leads to the increased release of exosomes in the vDG, which is reflected in the levels of neuronal exosomes isolated from plasma. Using the same chronic stress paradigm, prior studies showed that CRS leads to remodeling of apical hippocampal dendrites (31) and suppression of neurogenesis in the vDG (12), both dependent upon glutamate release acting synergistically with glucocorticoids (52). Prior work also showed a link between higher release of exosomes and increased synaptic glutamatergic transmission (20). Dysfunction of glutamatergic neurotransmission is a core feature of major mental illnesses (19). The CRS-induced increase in neuronal exosome levels in vDG together with the prior findings of suppressed expression of $mGlu_2$ receptors after chronic stress is akin to the role of exosomes in the regulation of multiple biological processes dependent upon glutamate overflow (12–14). The rapid amelioration of neuronal exosome levels assayed in plasma of CRS mice after administration of LAC supports a link between glutamatergic activity and exosome levels in responses to chronic stress. As we reviewed elsewhere, there are multiple biological mechanisms underlying the rapid antidepressant-like response of LAC that involve epigenetic modulation of glutamatergic function and its effects on the normalization of insulin resistance (12,15,16,53). It is also interesting to note the decrease in $NrCAM^+$ exosome levels in not-stressed mice receiving LAC that is akin to prior findings that showed a subset of more susceptible mice among not-stressed mice characterized by a predisposition to develop stress-induced neurobiological and behavioral deficits owing to a mineralocorticoid receptor–mediated suppression of $mGlu_2$ receptor among other factors (32,54). Future research is warranted to study individual differences in exosome levels among genetically similar mice with $NrCAM^+$ as a marker to detect more subtle changes. Lastly, the finding of the rapid amelioration of neuronal exosome levels after administration of LAC to CRS mice is of particular importance to translational research because of the previously reported finding of increased neuronal exosomes assayed in plasma of patients with MDD characterized by a deficiency of LAC (1). Regulation of neuronal exosome levels may represent an innovative therapeutic target in treatment of stress-related disorders, including depression, toward the development of more effective precision medicine models.

In contrast to the increased neuronal exosome levels in the vDG, our data showed that chronic stress led to a suppression of neuronal exosome levels in the BLA and that these effects paralleled the patterns of changes in transcriptomic profiles of these 2 brain areas. The higher levels of vDG neuronal exosomes were associated with an increased number of upregulated transcripts in this same brain area after CRS; conversely, the lower neuronal exosomes levels in the BLA were associated with an increased number of downregulated transcripts in this other key brain area. Bioinformatic analyses showed meaningful changes in molecular pathways related to dendritic remodeling, neuron projection, and extracellular matrix compartments. The divergent plasticity in terms of exosome levels between the vDG and BLA is akin to prior findings of opposite responses of these 2 brain areas to chronic stress in terms of morphology and synaptic and dendritic plasticity (13,23,31). Clinical studies have also shown smaller hippocampal volume in subjects with depression (55,56), whereas amygdala enlargement has been reported in children of mothers with chronic depression (57). Future studies are warranted on further development of the exosome technology to capture the response of the BLA with new markers for the isolation of the specific exosomes from plasma that may reflect changes in the BLA to add further regional granularity for this brain area.

It is interesting to note that β-estradiol signaling was the common upstream regulator pathway with the largest *z* score across the 2 areas with an opposite pattern of changes (upregulated in vDG, downregulated in BLA). This directionality of changes paralleled the pattern of changes observed in neuronal exosome levels. Our bioinformatic analysis showed that β-estradiol signaling was the only upstream regulator predicted to regulate synaptotagmins *Syt2* and *Syt6*, 2 transcripts responsible for the GO enrichment for secretory/exocytic vesicles. Prior work showing that exosome secretion is modulated by β-estradiol signaling support the current findings of β-estradiol signaling as a main driver of exosome levels in the stress response (43). It is also fascinating to note that previous work showed that β-estradiol protects neurons from the development of insulin resistance (58). Moreover, in the aftermath of the stress response, β-estradiol signaling acts synergistically with glutamatergic neurotransmission to modulate brain plasticity (12,13). The current work suggests a link between CRS-related exosome levels and β-estradiol signaling in the male mouse brain. Because of the known sex differences in the stress response and in β-estradiol signaling, including the source of β-estradiol in the brain that differs between male and female mice, the current findings support further exploration to characterize the connection between β-estradiol signaling and exosome biology in the stress response and understand potential sex differences in these biological processes.

Conclusions

In all, this work establishes a link between neuronal exosomes assayed in the hippocampus (vDG) and plasma, providing a conceptual template for future studies regarding new forms of brain-body communication to develop multidimensional models of resilience to stress. This work supports future studies aimed at ascertaining the exosome cargo that can have important translational and biomarker utility. Our findings also lay the groundwork for further exploration of the role of steroid and sex hormones in these processes. Together with prior findings of aberrant LAC levels and increased levels of

neuronal exosomes in patients with depression, we hope that this study will stimulate the opening of new therapeutic strategies targeted at adjusting neuronal exosome levels important for a variety of stress-related disorders.

ACKNOWLEDGMENTS AND DISCLOSURES

This work was supported by an award from the Hope for Depression Research Foundation and a fund from the Nathan Kline Institute for Psychiatric Research (to CN).

The authors report no biomedical financial interests or potential conflicts of interest.

ARTICLE INFORMATION

From the Department of Psychiatry, New York University Grossman School of Medicine, New York, New York (HK, SA, ASG, BB, CN); Nathan Kline Institute for Psychiatric Research, Orangeburg, New York (HK, AS, SA, ASG, BB, CN); Harold and Margaret Milliken Hatch Laboratory of Neuroendocrinology, the Rockefeller University, New York, New York (DZ, TL, JD, CN); Department of Neuroscience and Physiology, New York University Grossman School of Medicine, New York, New York (CN); and Neuroscience Institute, New York University Grossman School of Medicine, New York, New York (CN).

Address correspondence to Carla Nasca, Ph.D., at Carla.Nasca@nyulangone.org.

Received Feb 13, 2024; revised Sep 4, 2024; accepted Sep 8, 2024.

Supplementary material cited in this article is available online at https://doi.org/10.1016/j.bpsgos.2024.100401.

REFERENCES

1. Nasca C, Dobbin J, Bigio B, Watson K, de Angelis P, Kautz M, *et al.* (2021): Insulin receptor substrate in brain-enriched exosomes in subjects with major depression: On the path of creation of biosignatures of central insulin resistance. Mol Psychiatry 26:5140–5149.
2. Saeedi S, Israel S, Nagy C, Turecki G (2019): The emerging role of exosomes in mental disorders. Transl Psychiatry 9:122.
3. Couch Y, Akbar N, Davis S, Fischer R, Dickens AM, Neuhaus AA, *et al.* (2017): Inflammatory stroke extracellular vesicles induce macrophage activation. Stroke 48:2292–2296.
4. Edwardson MA, Mitsuhashi M, Van Epps D (2024): Elevation of astrocyte-derived extracellular vesicles over the first month post-stroke in humans. Sci Rep 14:5272.
5. Kalluri R, LeBleu VS (2020): The biology, function, and biomedical applications of exosomes. Science 367:eaau6977.
6. O'Brien K, Breyne K, Ughetto S, Laurent LC, Breakefield XO (2020): RNA delivery by extracellular vesicles in mammalian cells and its applications. Nat. Rev. Mol. Cell Biol. 21:585–606.
7. Valadi H, Ekström K, Bossios A, Sjöstrand M, Lee JJ, Lötvall JO (2007): Exosome-mediated transfer of mRNAs and microRNAs is a novel mechanism of genetic exchange between cells. Nat. Cell Biol. 9:654–659.
8. Guay C, Regazzi R (2017): Exosomes as new players in metabolic organ cross-talk. Diabetes Obes Metab. 19(Suppl 1):137–146.
9. Zhang Y, Xu C (2022): Effects of exosomes on adult hippocampal neurogenesis and neuropsychiatric disorders. Mol Biol Rep 49:6763–6777.
10. Korkut C, Li Y, Koles K, Brewer C, Ashley J, Yoshihara M, Budnik V (2013): Regulation of postsynaptic retrograde signaling by presynaptic exosome release. Neuron 77:1039–1046.
11. Sharma P, Mesci P, Carromeu C, McClatchy DR, Schiapparelli L, Yates JR, *et al.* (2019): Exosomes regulate neurogenesis and circuit assembly. Proc Natl Acad Sci U S A 116:16086–16094.
12. McEwen BS, Bowles NP, Gray JD, Hill MN, Hunter RG, Karatsoreos IN, Nasca C (2015): Mechanisms of stress in the brain. Nat Neurosci 18:1353–1363.
13. McEwen BS, Nasca C, Gray JD (2016): Stress effects on neuronal structure: Hippocampus, amygdala, and prefrontal cortex. Neuropsychopharmacology 41:3–23.
14. Popoli M, Yan Z, McEwen BS, Sanacora G (2011): The stressed synapse: The impact of stress and glucocorticoids on glutamate transmission. Nat Rev Neurosci 13:22–37.
15. Nasca C, Bigio B, Zelli D, de Angelis P, Lau T, Okamoto M, *et al.* (2017): Role of the astroglial glutamate exchanger xCT in ventral hippocampus in resilience to stress. Neuron 96:402–413.e5.
16. Nasca C, Xenos D, Barone Y, Caruso A, Scaccianoce S, Matrisciano F, *et al.* (2013): L-acetylcarnitine causes rapid antidepressant effects through the epigenetic induction of mGlu2 receptors. Proc Natl Acad Sci U S A 110:4804–4809.
17. Nasca C, Bigio B, Lee FS, Young SP, Kautz MM, Albright A, *et al.* (2018): Acetyl-L-carnitine deficiency in patients with major depressive disorder. Proc Natl Acad Sci U S A 115:8627–8632.
18. Post RM (2018): Myriad of implications of acetyl-l-carnitine deficits in depression. Proc Natl Acad Sci U S A 115:8475–8477.
19. Akil H, Gordon J, Hen R, Javitch J, Mayberg H, McEwen B, *et al.* (2018): Treatment resistant depression: A multi-scale, systems biology approach. Neurosci Biobehav Rev 84:272–288.
20. Frühbeis C, Fröhlich D, Kuo WP, Amphornrat J, Thilemann S, Saab AS, *et al.* (2013): Neurotransmitter-triggered transfer of exosomes mediates oligodendrocyte-neuron communication. PLoS Biol 11:e1001604.
21. Friedrich MJ (2017): Depression is the leading cause of disability around the world. JAMA 317.. 1517–1517.
22. Kessler RC, Berglund P, Demler O, Jin R, Koretz D, Merikangas KR, *et al.* (2003): The epidemiology of major depressive disorder: Results from the National Comorbidity Survey Replication (NCS-R). JAMA 289:3095–3105.
23. Lau T, Bigio B, Zelli D, McEwen BS, Nasca C (2017): Stress-induced structural plasticity of medial amygdala stellate neurons and rapid prevention by a candidate antidepressant. Mol Psychiatry 22:227–234.
24. Lakshminarasimhan H, Chattarji S (2012): Stress leads to contrasting effects on the levels of brain derived neurotrophic factor in the hippocampus and amygdala. PLoS One 7:e30481.
25. Cuccurazzu B, Bortolotto V, Valente MM, Ubezio F, Koverech A, Canonico PL, Grilli M (2013): Upregulation of mGlu2 receptors via NF-κB p65 acetylation is involved in the proneurogenic and antidepressant effects of acetyl-L-carnitine. Neuropsychopharmacology 38:2220–2230.
26. GTEx Consortium (2013): The Genotype-Tissue Expression (GTEx) project. Nat Genet 45:580–585.
27. Takahashi H, Lassmann T, Murata M, Carninci P (2012): 5′ end–centered expression profiling using cap-analysis gene expression and next-generation sequencing. Nat Protoc 7:542–561.
28. Uhlén M, Fagerberg L, Hallström BM, Lindskog C, Oksvold P, Mardinoglu A, *et al.* (2015): Proteomics. Tissue-based map of the human proteome. Science 347:1260419.
29. Zhang Y, Chen K, Sloan SA, Bennett ML, Scholze AR, O'Keeffe S, *et al.* (2014): An RNA-sequencing transcriptome and splicing database of glia, neurons, and vascular cells of the cerebral cortex. J Neurosci 34:11929–11947.
30. Yao Z, van Velthoven CTJ, Nguyen TN, Goldy J, Sedeno-Cortes AE, Baftizadeh F, *et al.* (2021): A taxonomy of transcriptomic cell types across the isocortex and hippocampal formation. Cell 184:3222–3241.e26.
31. Magariños AM, McEwen BS (1995): Stress-induced atrophy of apical dendrites of hippocampal CA3c neurons: Involvement of glucocorticoid secretion and excitatory amino acid receptors. Neuroscience 69:89–98.
32. Nasca C, Menard C, Hodes G, Bigio B, Pena C, Lorsch Z, *et al.* (2019): Multidimensional predictors of susceptibility and resilience to social defeat stress. Biol Psychiatry 86:483–491.
33. Peña CJ, Kronman HG, Walker DM, Cates HM, Bagot RC, Purushothaman I, *et al.* (2017): Early life stress confers lifelong stress susceptibility in mice via ventral tegmental area OTX2. Science 356:1185–1188.
34. Nasca C, Zelli D, Bigio B, Piccinin S, Scaccianoce S, Nisticò R, McEwen BS (2015): Stress dynamically regulates behavior and glutamatergic gene expression in hippocampus by opening a window of epigenetic plasticity. Proc Natl Acad Sci U S A 112:14960–14965.
35. Moda-Sava RN, Murdock MH, Parekh PK, Fetcho RN, Huang BS, Huynh TN, *et al.* (2019): Sustained rescue of prefrontal circuit dysfunction by antidepressant-induced spine formation. Science 364:eaat8078.
36. McEwen BS (2010): Stress, sex, and neural adaptation to a changing environment: Mechanisms of neuronal remodeling. Ann N Y Acad Sci 1204(suppl):E38–E59.
37. Bigio B, Mathé AA, Sousa VC, Zelli D, Svenningsson P, McEwen BS, Nasca C (2016): Epigenetics and energetics in ventral hippocampus

mediate rapid antidepressant action: Implications for treatment resistance. Proc Natl Acad Sci U S A 113:7906–7911.
38. Pfaff DW (1980): Estrogens and Brain Function. In: Neural Analysis of a Hormone-Controlled Mammalian Reproductive Behavior. New York: Springer.
39. McEwen BS (1994): Steroid hormone actions on the brain: When is the genome involved? Horm Behav 28:396–405.
40. Lee SJ, McEwen BS (2001): Neurotrophic and neuroprotective actions of estrogens and their therapeutic implications. Annu Rev Pharmacol Toxicol 41:569–591.
41. Wei J, Yuen EY, Liu W, Li X, Zhong P, Karatsoreos IN, *et al.* (2014): Estrogen protects against the detrimental effects of repeated stress on glutamatergic transmission and cognition. Mol Psychiatry 19:588–598.
42. Foy MR, Baudry M, Foy JG, Thompson RF (2008): 17beta-estradiol modifies stress-induced and age-related changes in hippocampal synaptic plasticity. Behav Neurosci 122:301–309.
43. Drula R, Pardini B, Fu X, De Los Santos MC, Jurj A, Pang L, *et al.* (2023): 17β-estradiol promotes extracellular vesicle release and selective miRNA loading in ERα-positive breast cancer. Proc Natl Acad Sci U S A 120:e2122053120.
44. Ishii M, Senju A, Oguro A, Shimono M, Araki S, Kusuhara K, *et al.* (2020): Measurement of the estradiol concentration in cerebrospinal fluid from infants and its correlation with serum estradiol and exosomal MicroRNA-126-5p. Biol Pharm Bull 43:1966–1968.
45. Agrawal R, Reno CM, Sharma S, Christensen C, Huang Y, Fisher SJ (2021): Insulin action in the brain regulates both central and peripheral functions. Am J Physiol Endocrinol Metab 321:E156–E163.
46. Chen W, Cai W, Hoover B, Kahn CR (2022): Insulin action in the brain: Cell types, circuits, and diseases. Trends Neurosci 45:384–400.
47. Zarate CA, Machado-Vieira R (2017): Ketamine: Translating mechanistic discoveries into the next generation of glutamate modulators for mood disorders. Mol Psychiatry 22:324–327.
48. Rasgon NL, McEwen BS (2016): Insulin resistance-A missing link no more. Mol Psychiatry 21:1648–1652.
49. Duman RS, Li N (2012): A neurotrophic hypothesis of depression: Role of synaptogenesis in the actions of NMDA receptor antagonists. Philos Trans R Soc Lond B Biol Sci 367:2475–2484.
50. Raison CL, Miller AH (2011): Is depression an inflammatory disorder? Curr Psychiatry Rep 13:467–475.
51. Miller AH, Raison CL (2016): The role of inflammation in depression: From evolutionary imperative to modern treatment target. Nat Rev Immunol 16:22–34.
52. McEwen BS (2007): Physiology and neurobiology of stress and adaptation: Central role of the brain. Physiol Rev 87:873–904.
53. Bigio B, Azam S, Mathé AA, Nasca C (2024): The neuropsychopharmacology of acetyl-L-carnitine (LAC): Basic, translational and therapeutic implications. Discov Ment Health 4:2.
54. Nasca C, Bigio B, Zelli D, Nicoletti F (2015): Mind the gap: Glucocorticoids modulate hippocampal glutamate tone underlying individual differences in stress susceptibility. Mol Psychiatry 20:755–763.
55. Sheline YI, Liston C, McEwen BS (2019): Parsing the hippocampus in depression: Chronic stress, hippocampal volume, and major depressive disorder. Biol Psychiatry 85:436–438.
56. Barch DM, Tillman R, Kelly D, Whalen D, Gilbert K, Luby JL (2019): Hippocampal volume and depression among young children. Psychiatry Res Neuroimaging 288:21–28.
57. Lupien SJ, Parent S, Evans AC, Tremblay RE, Zelazo PD, Corbo V, *et al.* (2011): Larger amygdala but no change in hippocampal volume in 10-year-old children exposed to maternal depressive symptomatology since birth. Proc Natl Acad Sci U S A 108:14324–14329.
58. Qiu J, Bosch MA, Meza C, Navarro UV, Nestor CC, Wagner EJ, *et al.* (2018): Estradiol protects proopiomelanocortin neurons against insulin resistance. Endocrinology 159:647–664.